Research Square

Preprints are preliminary reports that have not undergone peer review.
They should not be considered conclusive, used to inform clinical practice,
or referenced by the media as validated information.

Experimental Investigation of the Effect of Reduced Graphene Oxide Coating on Copper Electrode Performance in Electrical Discharge Machining of X40CrMoV5 Steel

Mohammad Khosravi

mkhosravi@birjandut.ac.ir

Birjand University of Technology

Hossein Afshari

University of Birjand

Ali Mir

K. N. Toosi University of Technology

Article

Keywords: Electrical Discharge Machining (EDM), Coated electrode, Reduced Graphene Oxide (rGO), Design of Experiments (DOE)

Posted Date: November 24th, 2026

DOI: https://doi.org/10.21203/rs.3.rs-11440040/v1

License: This work is licensed under a Creative Commons Attribution 4.0 International License.
Read Full License

Additional Declarations: No competing interests reported.

Experimental Investigation of the Effect of Reduced Graphene Oxide Coating on Copper Electrode Performance in Electrical Discharge Machining of X40CrMoV5 Steel

Mohammad Khosravi[1*], Hossein Afshari[2], Ali Mir[3]

1 Department of mechanical and material engineering, Birjand University of Technology, Birjand, Iran
2 Department of mechanical engineering, University of Birjand, Birjand, Iran
3 Department of mechanical engineering, K. N. Toosi University of Technology, Tehran, Iran

ABSTRACT

The Electrical Discharge Machining (EDM) process is recognized as an advanced manufacturing method for fabricating parts with complex geometries and hard to cut materials. This study investigates the EDM process parameters using two types of electrodes: bare copper and reduced graphene oxide (RGO)-coated copper. To this end, the Box–Behnken design (BBD) under the Response Surface Methodology (RSM) framework is employed to examine the effects of process parameters on the Material Removal Rate (MRR), Tool Wear Rate (TWR), and Surface Roughness (SR) of machined X40CrMoV5 steel workpieces. The experimental results demonstrate that the RGO-coated electrode increases the material removal rate by up to 23.72% and reduces surface roughness by up to 12.5%. Furthermore, the tool wear rate for the coated electrode decreases by 87.07% compared to the conventional copper electrode. Among the investigated parameters, discharge current has the most significant influence on MRR, whereas voltage exhibits the greatest effect on surface roughness. Subsequently, multi-response optimization was carried out using the desirability function approach in Minitab software, and optimal levels for each parameter were determined. Overall, the application of a reduced graphene oxide coating on the copper electrode, coupled with process parameter optimization, substantially improves surface quality, enhances the material removal rate, and diminishes tool wear in the machining of X40CrMoV5 steel.

Keywords: Electrical Discharge Machining (EDM) - Coated electrode - Reduced Graphene Oxide (rGO) - Design of Experiments (DOE)

1. INTRODUCTION[1]

With the continuous expansion of manufacturing industries, the necessity of implementing advanced and diverse fabrication techniques has become more critical than ever. In this context, conventional machining processes encounter severe limitations when dealing with parts characterized by intricate geometries or manufactured from difficult to cut materials [1, 2].

Among advanced manufacturing technologies, Electrical Discharge Machining (EDM) has emerged as an effective non-traditional process enabling the fabrication of complex components with superior precision [3–5].

In EDM, material removal is achieved through a sequence of repetitive electrical spark discharges generated across a small gap between the tool and the workpiece, causing localized melting and vaporization of the material [6–9].

This thermoelectric mechanism enables the machining of any electrically conductive and semi conductive materials regardless of their mechanical properties. Moreover, a dielectric fluid is continuously supplied to cool the machining zone, flush debris, and facilitate localized ionization [10, 11].

Owing to distinctive features such as independence from workpiece hardness and mechanical strength, absence of direct mechanical contact forces, burr free surfaces, and the capability to generate sophisticated 3D features, EDM is widely utilized across mold and die manufacturing, automotive, aerospace, marine, and turbine industries [12–15].

In EDM operations, key performance metrics include material removal rate (MRR), tool wear rate (TWR), and surface roughness (SR). These indicators are predominantly dictated by operating parameters, including discharge current, gap voltage, pulse-on and pulse-off times, spark gap distance, and electrode material. Proper calibration and control of these factors are crucial to maximizing MRR while suppressing tool wear [16–20].

A major challenge during electrical discharge machining is progressive tool degradation. One effective route to bolster mechanical properties and wear resistance is the deposition of protective functional coatings on the electrode surface. A wear resistant surface coating mitigates thermal and electrical degradation, thereby prolonging tool life and dimensional fidelity [21].

Various coating routes, such as diffusion treatment, hot dipping, and electrodeposition, have been documented in the literature [22, 23].

Anthuvan et al. [24] explored MRR and TWR during EDM using copper electrodes. Multi response optimization yielded optimal operating values of 4 A discharge current, 2 μs pulse on time, and 4.6 μs pulse off time. Subsequently, these optimized conditions were applied to evaluate electrodes coated with conductive materials (silver, nickel, and zinc) as well as an insulating epoxy layer. Their findings indicated that each coating material uniquely promoted specific aspects of machining performance.

Extensive research has investigated parameter optimization in EDM systems. Naveed Ahmed et al. [25] examined surface roughness and microhardness of AISI 316L stainless steel machined using brass, copper, and aluminum electrodes. Process parameters namely peak current, pulse duration, pulse interval, and spark voltage were optimized. The lowest surface roughness (1.08 μm) was achieved with the aluminum electrode, whereas the highest microhardness (1270.6 HV) was attained using the brass tool. Microstructural characterization revealed that the aluminum electrode produced shallower and smaller discharge craters with fewer micro voids, whereas brass tools led to deep craters, microcracks, and pronounced surface topography.

Laibia and Shather [26] assessed MRR, SR, and tool erosion during the EDM of AISI 304 stainless steel using a copper-silicon carbide (Cu-SiC) composite electrode. Their investigated parameters included discharge currents of 1.5, 2, 3, 5, and 8 A, pulse intervals of 12 and 25 μs, and a 1 mm spark gap. The optimal surface finish occurred at 1.5 A and 25 μs, whereas the highest MRR was obtained at 8 A and 25 μs.

Similarly, Walia et al. [27] evaluated the surface integrity of AISI H13 tool steel machined with a porous Cu-TiC composite electrode, demonstrating that increases in peak current, pulse duration, and pulse interval consistently elevated workpiece surface roughness.

Electrode selection remains pivotal in determining EDM performance [28, 29]. Copper is predominantly favored for its high electrical and thermal conductivities, steel for mechanical rigidity, and brass for a balanced combination of conductivity and wear endurance. The electrode material exerts a governing influence on material removal kinetics, resulting surface integrity, and electrode degradation [30, 31].

Chiou et al. [32] comparatively assessed conventional tungsten carbide (WC), Ag-coated WC, and Cu-coated WC electrodes during the EDM of SKH59 high-speed tool steel. Their findings showed that the Ag-coated WC electrode yielded the lowest surface roughness, while the Cu-coated variant provided the highest MRR, followed by Ag-coated and bare WC tools, validating the beneficial role of conductive coatings on thermal and electrical discharge behavior.

Graphene, a two-dimensional carbon allotrope, has attracted significant research interest as an advanced coating material owing to its exceptional physical and mechanical properties. Graphene features superior electrical and thermal conductivities, high tensile strength, outstanding tribological performance, and high flexibility. These properties have enabled widespread adoption across microelectronics, nanocomposites, biomedical engineering, aerospace, machining, sporting goods,

wind turbine blades, and carbon nanotube architectures. Applied as an electrode surface modification, graphene enhances tool durability, improves spark channel efficiency, and suppresses localized thermal degradation [33, 34].

In EDM, MRR, TWR, and SR are governed by an interdependent set of variables, including discharge current, pulse-on time, pulse-off time, gap voltage, and tool material. A frequent detriment during machining is secondary sparking, which degrades surface topography and compromises dimensional tolerances. Applying a highly conductive protective coating serves as a viable remedy to eliminate arcing and secondary discharges by promoting stable spark ionization. In this study, the EDM behavior of X40CrMoV5 tool steel is investigated using both bare copper and reduced graphene oxide (RGO) coated copper electrodes. Employing a design of experiments (DOE) methodology, the direct and interactive effects of process parameters on MRR, TWR, and SR are systematically evaluated and compared across both electrode systems.

2. Materials and Methods

2.1. Materials and Tooling

In this study, the electrical discharge machining process was conducted using two categories of cylindrical tools: pure copper electrodes and reduced graphene oxide (RGO)-coated copper electrodes, each having a nominal diameter of 8 mm. Throughout the machining operations, the electrodes were connected to the positive terminal of the power generator, serving as the anode (positive tool polarity).

These two electrode configurations were selected to systematically evaluate the influence of tool material and surface coating on EDM performance characteristics, namely material removal rate, surface roughness, and tool erosion.

Optical emission spectrometry was performed according to the BS DIN EN 15079 standard to verify the elemental composition of the commercial grade pure copper stock; the measured chemical composition is detailed in Table 1.

Table 1. Chemical composition (wt.%) of the copper electrode

Cu	P	Te	Cr	Fe	Co
99.925	0.039	0.011	0.007	0.005	0.005

The workpieces were prepared from X40CrMoV5 steel. This alloy is extensively utilized in hot working dies and tooling applications owing to its favorable high temperature strength, excellent wear resistance, and thermal fatigue endurance. Test coupons were sectioned into uniform rectangular dimensions and subsequently surface-finished using a conventional manual lathe to ensure consistent initial surface conditions across all runs. The verified chemical composition of the X40CrMoV5 steel workpiece is summarized in Table 2.

Table 2. Chemical composition (wt.%) of X40CrMoV5 steel

Alloy	C	Si	Cr	Mo	V	Fe
Wt.%	0.4	1.0	5.30	1.40	1.0	Remainder

To carry out the electrical discharge machining (EDM) process, an Erosion Pishraneh 510 die-sinking EDM machine was employed. The adjustable voltage range of this machine is between 3 and 250 V. Furthermore, the machine features automatic motion along the Z-axis with a stroke of 270 mm, as well as manual movement along the X and Y axes with a vernier accuracy of 0.02 mm. Kerosene was utilized as the dielectric fluid to enhance flushing and debris evacuation from the machining zone.

2.2. Synthesis of Reduced Graphene Oxide Powder and Electrode Coating Process

Reduced graphene oxide (RGO) was synthesized from graphite precursor in a strongly acidic medium using a modified Hummers' method [35, 36]. During this process, the sample was centrifuged up to 15 times and sonicated for one hour to achieve adequate dispersion. In the final stage, the sample was

rinsed up to five times with double-distilled water. The resulting suspension was filtered until a semi solid state was obtained, and subsequently dried using a freeze drying method to preserve the structural integrity of the reduced graphene oxide. Specifically, the sample was maintained at 50 °C for 12 hours to remove surface adsorbed water.

To reduce graphene oxide (GO) to RGO, 200 mL of an aqueous GO suspension with a concentration of 2.5 g/L was initially prepared and dispersed under ultrasonic agitation for one hour. The solution was then transferred into an autoclave and maintained under hydrothermal conditions in an aqueous medium at 180 °C and a pressure of 12 bar for 12 hours. Finally, the resulting hydrogel was dried via freeze-drying to obtain the final product [37, 38].

Direct electrodeposition was utilized to fabricate the copper electrode coated with reduced graphene oxide. This technique is particularly suitable for coating electrically conductive components. First, the copper electrode was polished with fine emery paper (grit 1200) and cleaned in an ultrasonic bath containing acetone and deionized water for 5 minutes to eliminate surface contaminants. In this process, the workpiece is immersed in an electrolytic solution containing the coating materials, and a direct current (DC) is applied to the electrode via a power supply. Ions migrate from the electrolyte solution (anode) toward the workpiece surface (cathode), resulting in the deposition of a metallic or non-metallic layer. The properties and thickness of the deposited layer depend on parameters such as electrolyte composition, temperature, process duration, and current density.

In this study, RGO nanomaterials were prepared for substrate surface preparation using an electrolytic solution containing 1 vol% graphene oxide in water, with electrolysis performed at ambient temperature and atmospheric pressure.

This step was aimed at synthesizing high quality nanomaterials to coat the electrode surface and promote coating adhesion. Following nanomaterial preparation, the electrode was coated via direct electrodeposition under an applied voltage of 30 V and a current of 2 A for a duration of 60 minutes to achieve a uniform layer with adequate thickness. This coating process enhances electrical conductivity, improves wear resistance, and extends electrode tool life. Figure 1 illustrates the schematic stages of the electrode coating process employed in this study. Figure 1. Schematic diagram of the electrode coating process used in this study.

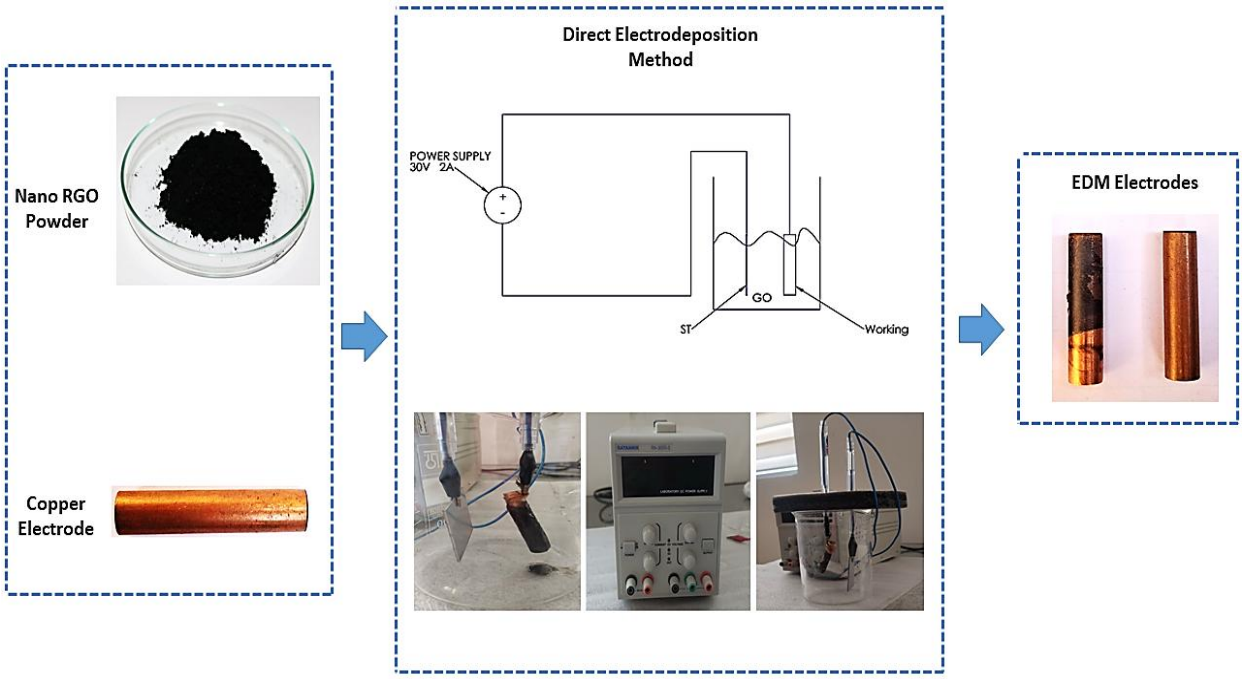


Figure 1. Schematic of the electrode coating procedure utilized in this work

2.3. Four-Point Probe Test

To accurately measure the electrical conductivity of both the bare copper and RGO-coated copper electrodes, the four-point probe method was employed. By eliminating the effect of contact resistance between the electrode and the measurement probes, this method provides superior accuracy compared to two probe techniques and is particularly suited for conductive materials and thin surface coatings. In this configuration, an electric current is supplied through the two outer probes, while the potential drop is measured across the two inner probes. Consequently, the resistivity and conductivity of the electrodes are calculated independently of contact resistance. The four point probe results enable a direct comparison between the conductivity of the bare copper electrode and the RGO-coated copper electrode, quantitatively demonstrating the role of the RGO coating in enhancing the tool's electrical properties.
Figure 2 displays the four point probe setup utilized for the electrodes evaluated in this research.

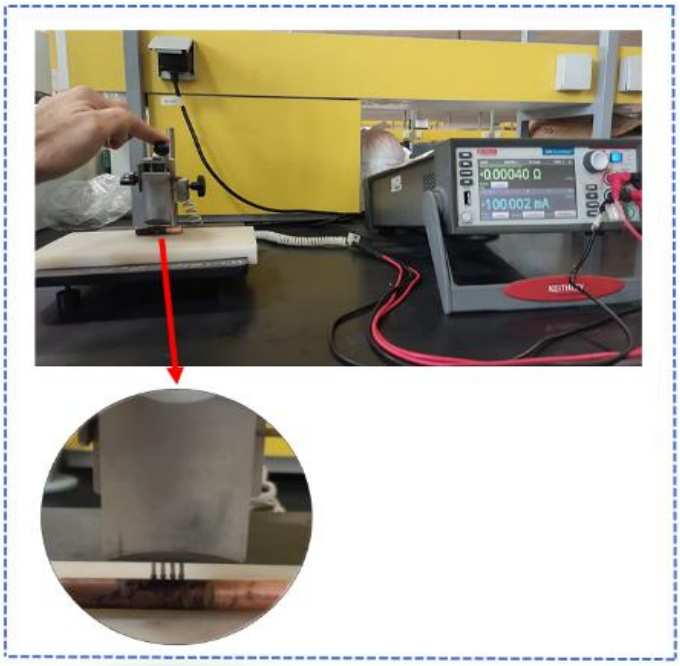


Figure 2. Four-point probe measurement setup

2.4. Design of Experiments (DoE)

Response surface methodology (RSM) is an efficient approach for process optimization that models the relationship between input parameters and output responses, thereby enabling the prediction of optimal operating conditions.
Among RSM techniques, the Box–Behnken design (BBD) is widely utilized due to requiring fewer experimental runs compared to other designs. This technique is categorized as an incomplete three level factorial design. In the Box Behnken design, combinations of two level factorial experiments are repeated in blocks across different sets of independent variables. The total number of runs is selected to minimize experimental cost and time while remaining sufficient to estimate the coefficients of a second-order polynomial model. Furthermore, the sensitivity of the output responses to uncontrollable factors and experimental noise is evaluated using the signal to noise (S/N) ratio [39, 40].
In this research, a Box Behnken RSM design was employed to analyze the process parameters and evaluate their effects on the material removal rate (MRR) of X40CrMoV5 tool steel, tool wear rate (TWR), and surface roughness (SR) of the EDM machined workpieces.
The variable continuous input parameters were selected as discharge voltage, peak current, pulse-on time, and pulse-off time. Three distinct levels were assigned to each parameter to capture any non-linear behavior in the process. The experiments were conducted using two electrode configurations:

a bare copper electrode and an RGO-coated copper electrode; hence, the electrode type was incorporated as a discrete factor in the experimental design.
According to this design, a total of 54 runs were performed. The design and statistical analysis were carried out using Minitab software. The selected levels for the investigated parameters are detailed in Table 3.

Table 3. Experimental factors and their levels in the design of experiments.

Parameter	Symbol	Level (+1)	Level (0)	Level (−1)
Voltage (V)	V	110	90	70
Discharge Current	I	8	5	2
Pulse-on Time (µs)	T_{on}	150	100	50
Pulse-off Time (µs)	T_{off}	75	50	25
Electrode Type	Electrode Type	—	RGO-Coated Copper	Pure Copper

It should be noted that the machining duration for all EDM runs was kept constant at 2 minutes.

2.5. Measurement of Material Removal Rate, Tool Wear, and Surface Roughness

The material removal rate (MRR) and tool wear rate (TWR) were calculated using Equations (1) and (2), respectively [9]:

$$\text{MRR} = \frac{(W_{P1} - W_{P2})}{\text{Time}} \quad (1)$$

$$\text{TWR} = \frac{(W_{T1} - W_{T2})}{\text{Time}} \quad (2)$$

Where MRR and TWR denote the material removal rate (g/min) and tool wear rate (g/min), respectively; W_{P1} and W_{P2} are the initial and final weights of the steel workpiece before and after the EDM process; W_{T1} and W_{T2} represent the initial and final weights of the tool electrode; and Time denotes the machining duration.
A digital balance (model DLS-100-6) was employed to accurately measure the masses of the workpieces and electrodes prior to and following the EDM operations. To assess the surface finish of the machined parts, surface roughness was measured using a Surtronic 3 stylus profilometer.This instrument evaluates the R_a parameter the arithmetic mean deviation of the surface roughness profile relative to the mean line which serves as the most widely used index for evaluating surface quality. Figure 3 illustrates the experimental procedure conducted in this investigation.



Figure 3. Schematic workflow of the experimental procedure in this study

Table 4 presents the experimental runs conducted based on the design of experiments in this study

Table 4. Experimental layout based on the design of experiments

NO.	T_{OFF} (µs)	T_{ON} (µs)	I (A)	V (v)	Electrode Type	Roughness (µm)	TWR (gr/min)	MRR (gr/min)
1	50	100	2	70	Copper	0.62	0.011420	0.002245
2	50	100	2	110	Copper	4.64	0.014560	0.002350
3	50	100	8	70	Copper	1.73	0.019540	0.124630
4	50	100	8	110	Copper	6.01	0.021150	0.113760
5	25	50	5	90	Copper	3.05	0.000850	0.065740
6	25	150	5	90	Copper	1.58	0.021530	0.009450
7	75	50	5	90	Copper	4.33	0.020520	0.079350
8	75	150	5	90	Copper	4.78	0.001350	0.018250
9	25	100	5	70	Copper	0.39	0.001630	0.043500
10	25	100	5	110	Copper	2.14	0.012430	0.026150
11	75	100	5	70	Copper	1.77	0.006920	0.058750
12	75	100	5	110	Copper	6.39	0.000850	0.054380
13	50	50	2	90	Copper	4.83	0.019750	0.007860
14	50	50	8	90	Copper	6.06	0.016520	0.204900
15	50	150	2	90	Copper	3.43	0.000150	0.002180
16	50	150	8	90	Copper	4.27	0.022640	0.067320
17	50	50	5	70	Copper	1.51	0.020340	0.087150
18	50	50	5	110	Copper	6.17	0.032580	0.094650
19	50	150	5	70	Copper	0.74	0.026785	0.021250
20	50	150	5	110	Copper	4.14	0.009650	0.014350
21	25	100	2	90	Copper	1.44	0.003940	0.004860
22	25	100	8	90	Copper	2.96	0.002140	0.131450
23	75	100	2	90	Copper	4.97	0.000900	0.002450
24	75	100	8	90	Copper	5.79	0.000210	0.131050
25	50	100	5	90	Copper	3.51	0.001050	0.002456
26	50	100	5	90	Copper	3.49	0.000640	0.002635
27	50	100	5	90	Copper	3.52	0.000350	0.001655
28	50	100	2	70	RGO Coated Copper	0.91	0.080640	0.001650
29	50	100	2	110	RGO Coated Copper	2.74	0.003320	0.001950
30	50	100	8	70	RGO Coated Copper	2.01	0.271408	0.183450
31	50	100	8	110	RGO Coated Copper	4.26	0.146450	0.176450

32	25	50	5	90	RGO Coated Copper	3.68	0.051600	0.083450
33	25	150	5	90	RGO Coated Copper	3.63	0.002380	0.045850
34	75	50	5	90	RGO Coated Copper	2.26	0.256530	0.094650
35	75	150	5	90	RGO Coated Copper	2.96	0.162460	0.028950
36	25	100	5	70	RGO Coated Copper	1.91	0.068250	0.079750
37	25	100	5	110	RGO Coated Copper	3.11	0.002187	0.057630
38	75	100	5	70	RGO Coated Copper	0.56	0.256350	0.063150
39	75	100	5	110	RGO Coated Copper	2.91	0.136430	0.051750
40	50	50	2	90	RGO Coated Copper	2.89	0.084750	0.000934
41	50	50	8	90	RGO Coated Copper	4.23	0.238460	0.236590
42	50	150	2	90	RGO Coated Copper	3.31	0.009760	0.004250
43	50	150	8	90	RGO Coated Copper	4.33	0.172460	0.119450
44	50	50	5	70	RGO Coated Copper	1.03	0.192460	0.094650
45	50	50	5	110	RGO Coated Copper	3.56	0.140350	0.082950
46	50	150	5	70	RGO Coated Copper	2.03	0.136430	0.042300
47	50	150	5	110	RGO Coated Copper	3.34	0.031670	0.022150
48	25	100	2	90	RGO Coated Copper	2.79	0.026210	0.000548
49	25	100	8	90	RGO Coated Copper	4.64	0.091420	0.163600
50	75	100	2	90	RGO Coated Copper	2.24	0.103410	0.001850
51	75	100	8	90	RGO Coated Copper	3.06	0.312480	0.163040
52	50	100	5	90	RGO Coated Copper	2.91	0.124650	0.001250
53	50	100	5	90	RGO Coated Copper	2.79	0.131670	0.001450
54	50	100	5	90	RGO Coated Copper	2.93	0.134280	0.001150

3. Results and Discussion

3.1. Four-Point Probe Test Results

The four point probe test results for both the bare copper and RGO-coated copper electrodes under a constant electrical current of 100.002 mA reveal that the resistance of the bare copper electrode (733×10^{-6} Ω) is approximately twice that of the RGO-coated copper electrode (380×10^{-6} Ω).
This substantial difference indicates an enhancement in electrical conductivity and a reduction in surface resistivity for the RGO-coated copper tool. In other words, the reduced graphene oxide coating significantly improves electrode performance by lowering electrical resistance and facilitating charge transfer.

3.2. Analysis of Variance (ANOVA)

Analysis of variance (ANOVA) was utilized to evaluate the significance and contribution of the input parameters toward the process output responses. Using statistical tests and mathematical models, ANOVA determines appropriate regression models for the investigated responses and quantifies the individual contribution and interaction effects of each factor [41, 42].
Tables 5 through 7 summarize the ANOVA results regarding the effects of the independent input parameters on the material removal rate (MRR) of X40CrMoV5 tool steel, tool wear rate (TWR), and surface roughness (R_a), respectively. A parameter is deemed statistically significant if its probability value (P-value) is less than 0.05.

Table 5. ANOVA results for the material removal rate of EDM-machined samples

Source	DF	Seq SS	Contribution	Adj MS	P-Value
Model	19	0.199156	98.92%	0.010482	0.000
Linear	5	0.158965	78.96%	0.031793	0.000
V (v)	1	0.000450	0.22%	0.000450	0.012
I (A)	1	0.132397	65.76%	0.132397	0.000

T_{ON} (µs)	1	0.022640	11.25%	0.022640	0.000
T_{OFF} (µs)	1	0.000053	0.03%	0.000053	0.369
Electrode Type	1	0.003425	1.70%	0.003425	0.000
Square	4	0.027992	13.90%	0.006998	0.000
$V(v)^2$	1	0.000579	0.29%	0.007723	0.000
$I(A)^2$	1	0.016048	7.97%	0.025243	0.000
$T_{ON}(\mu s)^2$	1	0.005057	2.51%	0.008746	0.000
T_{OFF} (µs)^3	1	0.006309	3.13%	0.006309	0.000
2-Way Interaction	10	0.012198	6.06%	0.001220	0.000
V (v)*I (A)	1	0.000042	0.02%	0.000042	0.424
V (v)*T_{ON} (µs)	1	0.000065	0.03%	0.000065	0.319
V (v)*T_{OFF} (µs)	1	0.000070	0.03%	0.000070	0.301
V (v)*Electrode Type	1	0.000067	0.03%	0.000067	0.312
I (A)*T_{ON} (µs)	1	0.007960	3.95%	0.007960	0.000
I (A)*T_{OFF} (µs)	1	0.000000	0.00%	0.000000	0.995
I (A)*Electrode Type	1	0.003272	1.63%	0.003272	0.000
T_{ON} (µs)*T_{OFF} (µs)	1	0.000135	0.07%	0.000135	0.154
T_{ON} (µs)*Electrode Type	1	0.000244	0.12%	0.000244	0.059
T_{OFF} (µs)*Electrode Type	1	0.000341	0.17%	0.000341	0.027
Error	34	0.002168	1.08%	0.000064	-
Lack-of-Fit	30	0.002167	1.08%	0.000072	0.000
Pure Error	4	0.000001	0.00%	0.000000	-
Total	53	0.201323	100.00%	-	-
R^2			**98.92%**		

Table 6. ANOVA results for the tool wear rate in the EDM process

Source	DF	Seq SS	Contribution	Adj MS	P-Value
Model	19	0.375563	98.35%	0.019766	0.000
Linear	5	0.274728	71.95%	0.054946	0.000
V (v)	1	0.012175	3.19%	0.012175	0.000
I (A)	1	0.038086	9.97%	0.038086	0.000
T_{ON} (µs)	1	0.009498	2.49%	0.009498	0.000
T_{OFF} (µs)	1	0.039515	10.35%	0.039515	0.000
Electrode Type	1	0.175454	45.95%	0.175454	0.000
Square	4	0.000748	0.20%	0.000187	0.415
$V(v)^2$	1	0.000023	0.01%	0.000041	0.639
$I(A)^2$	1	0.000204	0.05%	0.000157	0.363
$T_{ON}(\mu s)^2$	1	0.000321	0.08%	0.000149	0.376
$T_{OFF}(\mu s)^2$	1	0.000200	0.05%	0.000200	0.306
2-Way Interaction	10	0.100087	26.21%	0.010009	0.000
V (v)*I (A)	1	0.000302	0.08%	0.000302	0.210
V (v)*T_{ON} (µs)	1	0.000841	0.22%	0.000841	0.040
V (v)*T_{OFF} (µs)	1	0.000625	0.16%	0.000625	0.075
V (v)*Electrode Type	1	0.012591	3.30%	0.012591	0.000
I (A)*T_{ON} (µs)	1	0.000151	0.04%	0.000151	0.373
I (A)*T_{OFF} (µs)	1	0.002627	0.69%	0.002627	0.001
I (A)*Electrode Type	1	0.033235	8.70%	0.033235	0.000
T_{ON} (µs)*T_{OFF} (µs)	1	0.000897	0.23%	0.000897	0.034
T_{ON} (µs)*Electrode Type	1	0.007369	1.93%	0.007369	0.000
T_{OFF} (µs)*Electrode Type	1	0.041449	10.85%	0.041449	0.000
Error	34	0.006283	1.65%	0.000185	-
Lack-of-Fit	30	0.006233	1.63%	0.000208	0.007
Pure Error	4	0.000050	0.01%	0.000012	-
Total	53	0.381847	100.00%	-	-

R^2	98.35%

Table 7. ANOVA results for the surface roughness of EDM-machined samples

Source	DF	Seq SS	Contribution	Adj MS	P-Value
Model	19	117.377	97.34%	6.1777	0.000
Linear	5	68.885	57.12%	13.7770	0.000
V (v)	1	48.735	40.41%	48.7350	0.000
I (A)	1	8.809	7.30%	8.8088	0.000
T_{ON} (µs)	1	1.067	0.88%	1.0668	0.002
T_{OFF} (µs)	1	4.770	3.96%	4.7704	0.000
Electrode Type	1	5.504	4.56%	5.5040	0.000
Square	4	15.056	12.49%	3.7639	0.000
$V(v)^2$	1	9.926	8.23%	5.6292	0.000
$I(A)^2$	1	2.569	2.13%	2.6114	0.000
$T_{ON}(\mu s)^2$	1	2.209	1.83%	1.4488	0.000
$T_{OFF}(\mu s)^3$	1	0.351	0.29%	0.3512	0.062
2-Way Interaction	10	33.436	27.73%	3.3436	0.000
V (v)*I (A)	1	0.058	0.05%	0.0578	0.440
V (v)*T_{ON} (µs)	1	0.769	0.64%	0.7688	0.007
V (v)*T_{OFF} (µs)	1	2.020	1.68%	2.0201	0.000
V (v)*Electrode Type	1	5.283	4.38%	5.2828	0.000
I (A)*T_{ON} (µs)	1	0.063	0.05%	0.0630	0.420
I (A)*T_{OFF} (µs)	1	0.374	0.31%	0.3741	0.055
I (A)*Electrode Type	1	0.024	0.02%	0.0241	0.617
T_{ON} (µs)*T_{OFF} (µs)	1	0.891	0.74%	0.8911	0.004
T_{ON} (µs)*Electrode Type	1	3.345	2.77%	3.3451	0.000
T_{OFF} (µs)*Electrode Type	1	20.609	17.09%	20.6091	0.000
Error	34	3.213	2.66%	0.0945	-
Lack-of-Fit	30	3.201	2.65%	0.1067	0.002
Pure Error	4	0.012	0.01%	0.0030	-
Total	53	120.589	100.00%	-	-
R^2			**97.34%**		

Linear and multiple regression analyses are among the most versatile and effective statistical approaches for data interpretation, providing predictive mathematical relationships between the independent process variables and the responses. The implementation of regression analysis requires validating key statistical assumptions, including homogeneity of variance, normality of residuals, data independence, and normally distributed errors [43, 44]. The coefficient of determination (R^2) was evaluated to assess the predictive capability of the developed models. As shown in the ANOVA tables, the R2R^2R2 values are close to 100%, demonstrating that the derived models reliably predict MRR, TWR, and surface roughness for the machined X40CrMoV5 steel samples. Tables 8 through 10 present the regression equations obtained for MRR, TWR, and surface roughness, respectively.

Table 8. Regression equations for the material removal rate of EDM-machined X40CrMoV5 steel

Electrode Type			Equations
Copper	MRR	=	0.7128- 0.01206 V (v)- 0.00874 I (A)- 0.001496 T_{ON} (µs)- 0.003886T_{OFF}(µs)+ 0.000067 V (v)*V (v)+ 0.005405 I $(A)^2$+ 0.000011 T_{ON} $(\mu s)^2$+ 0.000039 $T_{OFF}(\mu s)^2$- 0.000038 V (v)* I (A) - 0.000003 V (v)*T_{ON}(µs) + 0.000006 V (v)*T_{OFF}(µs) - 0.000210 I (A)*T_{ON}(µs) + 0.000000 I (A)*T_{OFF}(µs) - 0.000003 T_{ON} (µs)*T_{OFF} (µs)

RGO Coated Copper	MRR	=	0.7072 - 0.01223 V (v) - 0.00096 I (A) - 0.001368 T_{ON}(µs)- 0.004188 T_{OFF}(µs) + 0.000067 V(v)^2+ 0.005405 I(A)^2 + 0.000011 T_{ON}(µs)^2 + 0.000039 T_{OFF}(µs)^2 - 0.000038 V (v)*I (A) - 0.000003 V (v)*T_{ON} (µs) + 0.000006 V (v)*T_{OFF} (µs) - 0.000210 I (A)*T_{ON} (µs) + 0.000000 I (A)*T_{OFF} (µs) - 0.000003 T_{ON} (µs)*T_{OFF} (µs)

Table 9. Regression equations for tool wear rate during the EDM process

Electrode Type	Equations		
Copper	TWR	=	-0.128+ 0.00155 V (v) - 0.00915 I (A) + 0.000856 T-ON (µs) + 0.00188 T-OFF (µs) + 0.000005 V (v)*V (v)+ 0.000427 I (A)*I (A)+ 0.000001 T-ON (µs)*T-ON (µs) - 0.000007 T-OFF (µs)*T-OFF (µs) - 0.000102 V (v)*I (A)- 0.000010 V (v)*T-ON (µs) - 0.000018 V (v)*T-OFF (µs) + 0.000029 I (A)*T-ON (µs) + 0.000242 I (A)*T-OFF (µs) - 0.000008 T-ON (µs)*T-OFF (µs)
RGO Coated Copper	TWR	=	-0.028 - 0.00074 V (v) + 0.01566 I (A) + 0.000155 T_{ON} (µs) + 0.00521 T_{OFF} (µs) + 0.000005 V (v)^2+ 0.000427 I (A)^2+ 0.000001 T_{ON}(µs)^2- 0.000007 T_{OFF} (µs)^2- 0.000102 V (v)*I (A) - 0.000010 V (v)*T_{ON} (µs) - 0.000018 V (v)*T_{OFF} (µs) + 0.000029 I (A)*T_{ON} (µs) + 0.000242 I (A)*T_{OFF} (µs)- 0.000008 T_{ON} (µs)*T_{OFF} (µs)

Table 10. Regression equations for surface roughness of the EDM-machined surfaces

Electrode Type	Equations		
Copper	Roughness	=	-17.45+ 0.3953 V(v)- 0.283 I(A)- 0.0237 T_{ON}(µs)- 0.0188 T_{OFF} (µs) - 0.001816 V (v)^2 + 0.0550 I (A)^2+ 0.000147 T_{ON} (µs)^2- 0.000290 T_{OFF}(µs)+ 0.00142 V (v)*I (A)- 0.0003 10 V (v)*T_{ON} (µs)+ 0.001005 V (v)*T_{OFF} (µs)- 0.000592 I (A)*T_{ON} (µs)- 0.00288 I (A) *T_{OFF}(µs) + 0.000267 T_{ON} (µs)*T_{OFF} (µs)
RGO Coated Copper	Roughness	=	-11.75+ 0.3484 V(v) - 0.261 I(A) - 0.0087 T_{ON}(µs) - 0.0929 T_{OFF}(µs) - 0.001816 V(v)^2 + 0.0550 I(A)^2+0.000147 T_{ON} (µs)^2- 0.000290 T_{OFF} (µs)^2+ 0.00142 V (v)*I (A)- 0.0003 10 V (v)*T_{ON} (µs)+ 0.001005 V (v)*T_{OFF} (µs)- 0.000592 I (A)*T_{ON} (µs)- 0.00288 I (A) *T_{OFF} (µs) + 0.000267 T_{ON} (µs)*T_{OFF} (µs)

Figures 4 to 6 illustrate the main effects of the input parameters on the material removal rate, tool wear rate, and surface roughness of the EDM machined X40CrMoV5 steel workpieces.

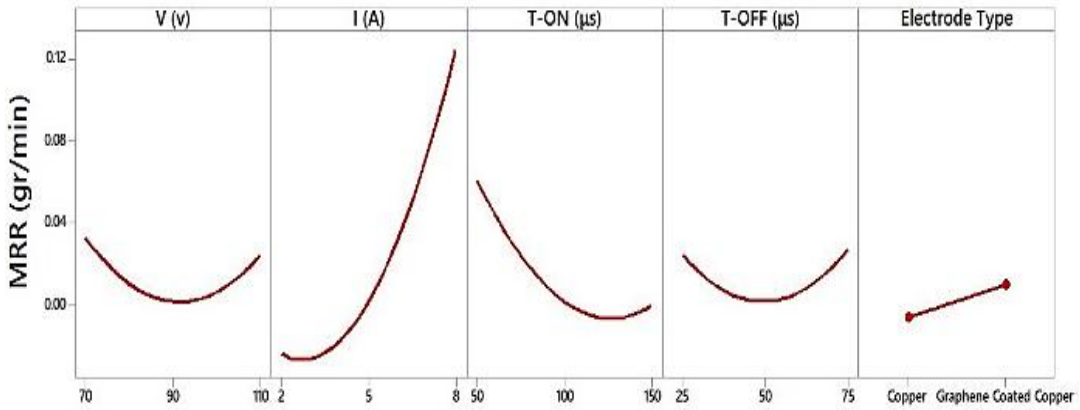


Figure 4. Effects of input parameters on the material removal rate of X40CrMoV5 steel

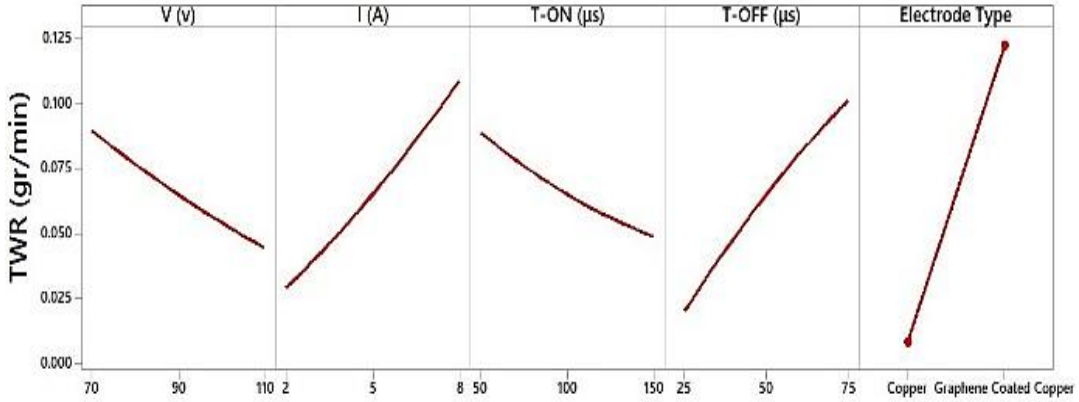


Figure 5. Effects of input parameters on the tool wear rate

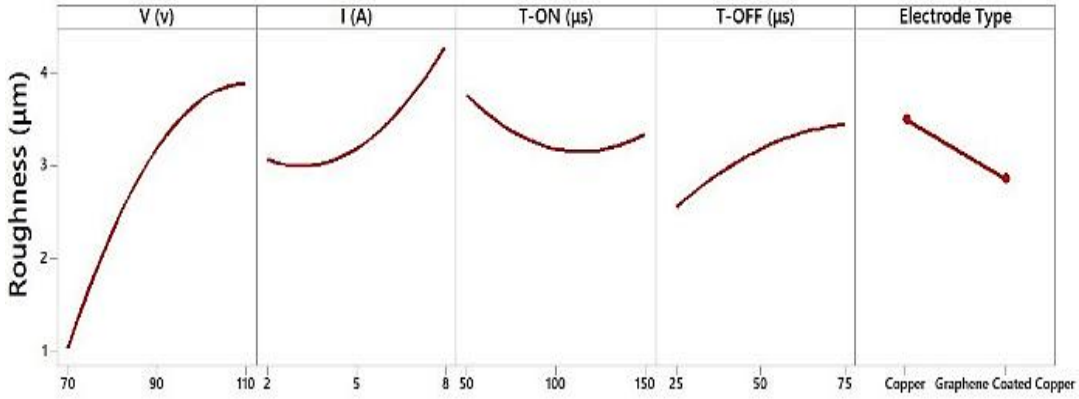


Figure 6. Effects of input parameters on the surface roughness of machined samples

Based on the results presented in Figure 4, discharge current is the most dominant factor governing the material removal rate in EDM. Increasing the current up to 8 A leads to a consistent upward trend in MRR. Conversely, an increase in pulse-on time reduces the material removal rate. According to Table 5, variations in voltage and pulse off time have no statistically significant impact on MRR. Comparing the two electrode configurations reveals that the RGO-coated copper electrode achieves higher material removal rates than the conventional bare copper electrode.

As depicted in Figure 5, increasing both the discharge current and the pulse off time increases the tool wear rate, which correlates directly with the elevated material removal rate. In other words, higher machining rates intensify thermal erosion on the tool electrode, thereby accelerating wear and reducing tool life. An increase in voltage, however, leads to a decrease in tool wear rate. Furthermore, extending the pulse on time up to 150 µ\muµs decreases tool wear. The experimental results also indicate that the RGO-coated copper electrode experiences higher wear compared to the bare copper electrode, which can be attributed to the physical characteristics of the RGO coating, particularly its high thermal conductivity and rapid heat transfer.

Figure 6 demonstrates that discharge voltage exerts the strongest influence on the surface roughness of the EDM machined parts. Increasing the voltage leads to a noticeable increase in surface roughness, primarily due to the higher spark discharge energy delivered per pulse. Furthermore, an increase in discharge current, especially beyond 5 A, further deteriorates surface finish by increasing roughness. In contrast, increasing the pulse-off time reduces the surface roughness of the machined specimens, which is likely associated with improved dielectric deionization and more uniform discharge occurrences. As inferred from Table 7, variations in pulse-on time have no significant effect

on surface roughness. Finally, a comparison between the two tools indicates that the bare copper electrode produces higher surface roughness than the RGO-coated copper electrode, demonstrating that the RGO coating promotes a smoother surface finish.

3.3. Multi-Objective Parameter Optimization

To simultaneously maximize the material removal rate, minimize the tool wear rate, and minimize surface roughness during the electrical discharge machining (EDM) process, multi-response optimization of the independent input parameters was conducted using the Response Optimizer tool in Minitab 18. In this regard, the desirability function approach was employed to determine the optimal parameter settings based on the estimated regression models.

In the desirability function approach, the predicted regression model for each response (y) is converted into an individual desirability function (d).

The value of ddd ranges between 0 and 1, where d=1 represents the ideal response state and d=0 indicates an unacceptable response beyond the specified constraints. Depending on the optimization objective, individual desirability can be formulated based on three criteria: (i) larger the better, (i) smaller the better, and (i) target is best. In the present study, the larger-the-better criterion is formulated using Equation (3) [45, 46]:

$$\begin{cases} 0 & y < L \\ \left(\frac{y-L}{T-L}\right)^r & \mathrm{L} \le \mathrm{y} \le T \\ 1 & y > T \end{cases} \quad (3)$$

where T and L denote the target value and the lower limit of the response, respectively, and r is the weight (importance exponent) assigned to the response, which is typically set to unity (r =1).

The composite desirability (D) is computed as the geometric mean of the individual desirability functions (d_i). In this study, the three output responses MRR, TWR, and surface roughness (R_a) were integrated into a single composite desirability index (D) using Equation (4) [47]:

$$\mathrm{D}=\sqrt[3]{\mathrm{d}_1\,(\mathrm{MRR}) \times \mathrm{d}_2\,(\mathrm{TWR}) \times \mathrm{d}_3\,(\mathrm{Roughness})} \quad (4)$$

where d_n represents the individual desirability for each response and D is the overall composite desirability. Table 11 summarizes the predicted optimal conditions alongside the experimental validation results.

Table 11. Multi-response optimization settings and experimental validation results

			Predicted Value (Minitab)	Experimental Value	Error (%)
Response	MRR (g/min)	Copper	0. 2281	0.2255	1.15
		RGO Coated Copper	0.2644	0.2790	5.23
	TWR (g/min)	Copper	0.0141	0.0147	4.08
		RGO Coated Copper	0.0283	0.0275	2.98
	Roughness (µm)	Copper	2.6057	2.6904	3.15
		RGO Coated Copper	2.2222	2.3540	5.69
Optimal Input Parameters		V = 70 v	I = 8 A	T_{on} = 50 µs	T_{off} = 50 µs

Figure 7 illustrates the performance responses under the optimized parameter settings for both the pure copper and RGO-coated copper electrodes.

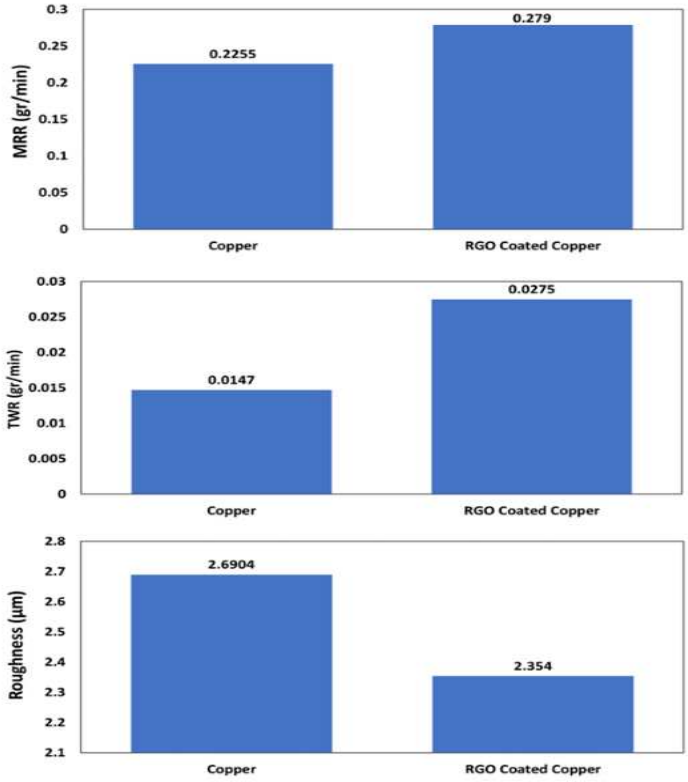


Figure 7. Comparison of performance responses under optimal machining parameters for different electrode types

Comparing the output responses in Figure 7 indicates that the RGO-coated copper tool is a superior choice for EDM of X40CrMoV5 tool steel, providing higher material removal rates and lower surface roughness. Applying the RGO coating to the copper electrode increased the material removal rate by 23.72% while reducing the tool wear rate and surface roughness by 87.07% and 12.50%, respectively, compared to baseline conditions.

3.4. SEM and EDS Analysis

Figure 8 presents scanning electron microscopy (SEM) micrographs of the RGO coated copper electrode surface following EDM processing. The microscopic examinations closely align with the experimental findings for material removal rate and tool wear. The preservation of the layered/sheet-like structure of the RGO coating on the electrode surface after machining highlights the high thermal stability of this nanocoating under transient electrical discharge thermal shocks.

The layered architecture of the RGO sheets effectively prevents extensive direct melting of the copper substrate (which has a substantially lower melting point than graphene). This behavior demonstrates the function of the RGO coating as an efficient heat dissipating barrier that prevents excessive thermal penetration into the bulk electrode, thereby suppressing the tool wear rate. Concurrently, the nanoscale pores and sharp edges of the RGO nanosheets promote rapid dielectric ionization and stabilize the plasma channel, enhancing spark efficiency and boosting the material removal rate. Furthermore, the uniform dispersion of discharge energy across the RGO sheets prevents deep localized crater formation on the electrode surface, leading to improved surface finish and reduced

roughness. At higher magnifications, fine details of the discharge coating interaction are evident. Smooth melted regions alongside porous zones indicate the formation of a recast layer where exfoliated RGO sheets have bonded with resolidified copper to form a composite surface architecture. The fine micro-voids act as micro reservoirs that trap dielectric fluid, aiding spark stability and assisting debris expulsion from the inter-electrode gap.

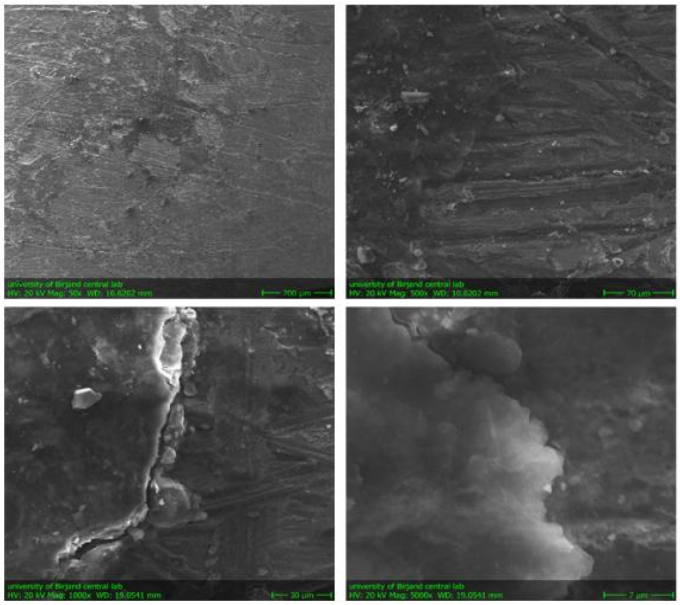


Figure 8. SEM micrographs of the RGO-coated copper electrode surface after the EDM process

To verify the elemental composition of the RGO-coated copper electrode, energy-dispersive X-ray spectroscopy (EDS) was performed. Figure 9 shows the EDS spectra obtained at two distinct locations on the electrode surface after machining.

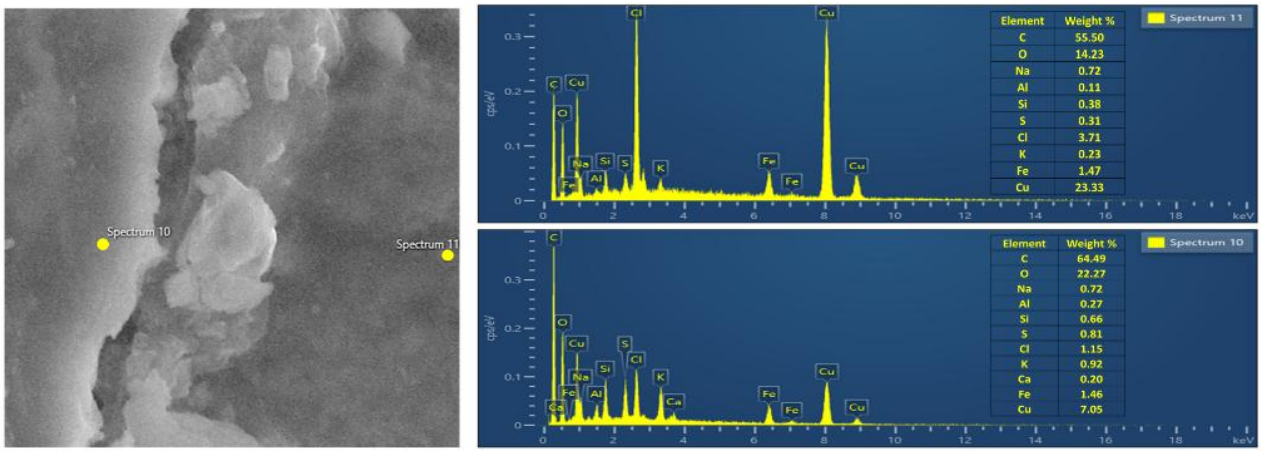


Figure 9. EDS spectra recorded at two distinct spots on the electrode surface after EDM

As shown in Figure 9, the prominent carbon and oxygen peaks in both spectra confirm the durability and retention of the RGO coating on the copper substrate despite the intense thermal conditions of EDM. At Spot 10, the relatively low copper concentration compared to carbon indicates the formation of a thick protective carbonaceous shield that prevents the plasma column from impinging directly onto the substrate, which explains the substantial reduction in tool wear rate observed experimentally.

The detection of iron (Fe) peaks further confirms workpiece-to-tool mass transfer during thermal discharge.
Figure 10. presents SEM micrographs of the workpiece surface machined with the RGO-coated copper electrode under the optimized operating parameters

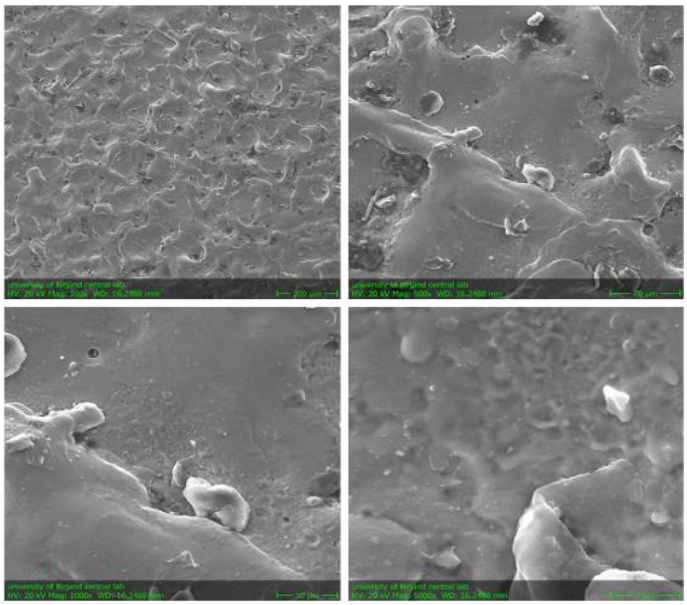


Figure 10. SEM micrographs of the workpiece surface machined using the RGO-coated copper electrode under optimal parameter settings

Figure 10 reveals a marked improvement in surface topography. At lower magnification, a uniform distribution of shallow discharge craters is observed, corroborating the lower surface roughness achieved with the RGO-coated electrode. The RGO nanosheets dissipate discharge energy over a wider surface area, preventing localized thermal concentration and deep crater formation. At higher magnification, the workpiece surface is virtually free of macroscopic gas cavities and severe microcracks. This morphology is attributed to the superior thermal dissipation and solid lubrication characteristics of the RGO nanosheets. The absence of extensive network microcracking at high magnification demonstrates enhanced surface structural integrity.

4. Conclusion

Electrical discharge machining (EDM) is a primary manufacturing technique for shaping hard to cut materials and complex geometric profiles. Key performance indicators namely material removal rate (MRR), tool wear rate (TWR), and surface roughness (R_a) are directly governed by the pulse parameters and electrode properties.
This study investigated the influence of tool surface modification using a reduced graphene oxide (RGO) coating alongside the optimization of EDM parameters during the machining of X40CrMoV5 hot-work tool steel.
The primary conclusions drawn from the experimental trials, statistical analyses, and optimization procedure are summarized as follows:

- Applying a reduced graphene oxide (RGO) coating to the copper electrode increases electrical conductivity by approximately twofold relative to bare copper.

- The maximum material removal rate (0.23659 g/min) was achieved using the RGO-coated copper electrode at an applied voltage of 90 V, a discharge current of 8 A, a pulse on time of 50 μs, and a pulse-off time of 50 μs.
- The lowest tool wear rate (0.00015 g/min) was recorded for the pure copper electrode at 90 V voltage, 2 A discharge current, 150 μs pulse-on time, and 50 μs pulse-off time.
- The minimum surface roughness (R_a=0.39 μm) was attained with the pure copper electrode under 70 V voltage, 5 A discharge current, 100 μ\muμs pulse on time, and 25 μ\muμs pulse off time.
- Implementing the RGO coating on the copper electrode yielded a 23.72% increase in material removal rate, an 87.07% reduction in tool wear rate, and a 12.50% improvement in surface roughness under multi objective optimized conditions.

Funding Declaration

This research received no specific grant from any funding agency.

Data availability statement

The data presented in this study are available on request from the corresponding author.

REFERENCES

[1] A. Elkaseer, A. Abdelaziz, M. Saber, and A. Nassef, "FEM-based study of precision hard turning of stainless steel 316L," Materials, vol. 12, no. 16, p. 2522, 2019.

[2] A. W. Alshaer, R. Abdallah, F. H. Rajab, A. A. Barzinjy, and O. B. Otanocha, "Understanding the machined material's behaviour in electro-discharge machining (EDM) using a multi-phase smoothed particle hydrodynamics (SPH) modelling," The International Journal of Advanced Manufacturing Technology, vol. 134, no. 1, pp. 369-387, 2024.

[3] J. E. Abu Qudeiri, A. Saleh, A. Ziout, A.-H. I. Mourad, M. H. Abidi, and A. Elkaseer, "Advanced electric discharge machining of stainless steels: Assessment of the state of the art, gaps and future prospect," Materials, vol. 12, no. 6, p. 907, 2019.

[4] J. E. A. Qudeiri, A. Zaiout, A.-H. I. Mourad, M. H. Abidi, and A. Elkaseer, "Principles and characteristics of different EDM processes in machining tool and die steels," Applied sciences, vol. 10, no. 6, p. 2082, 2020.

[5] K. Mouralova, J. Bednar, L. Benes, T. Plichta, T. Prokes, and J. Fries, "Production of precision slots in copper foil using micro EDM," Scientific reports, vol. 12, no. 1, p. 5023, 2022.

[6] R. Świercz, D. Oniszczuk-Świercz, and T. Chmielewski, "Multi-response optimization of electrical discharge machining using the desirability function," Micromachines, vol. 10, no. 1, p. 72, 2019.

[7] A. Molinetti, F. L. Amorim, P. C. Soares, and T. Czelusniak, "Surface modification of AISI H13 tool steel with silicon or manganese powders mixed to the dielectric in electrical discharge machining process," The International Journal of Advanced Manufacturing Technology, vol. 83, pp. 1057-1068, 2016.

[8] K. Mausam, P. K. Singh, K. Sharma, and R. Gupta, "Investigation of process parameter of EDM using genetic algorithm (GA) approach for carbon fiber based two phase epoxy composites," Materials Today: Proceedings, vol. 3, no. 10, pp. 4102-4108, 2016.

[9] K. Mausam, K. Sharma, G. Bharadwaj, and R. P. Singh, "Multi-objective optimization design of die-sinking electric discharge machine (EDM) machining parameter for CNT-reinforced carbon fibre nanocomposite using grey relational analysis," Journal of the Brazilian Society of Mechanical Sciences and Engineering, vol. 41, pp. 1-8, 2019.

[10] S. R. Jana, J. Shiek, and M. Ponnusamy, "Green dielectric exploration: spectrographic analysis and technical feasibility of vegetable oils in EDM via PIV, TOPSIS, and MOORA evaluation methods," Discover Applied Sciences, vol. 6, no. 10, p. 549, 2024.

[11] M. Y. Khan, P. S. Rao, and B. Pabla, "Investigations on the feasibility of Jatropha curcas oil based biodiesel for sustainable dielectric fluid in EDM process," Materials Today: Proceedings, vol. 26, pp. 335-340, 2020.

[12] P. Kumar, M. Gupta, and V. Kumar, "Surface integrity analysis of WEDMed specimen of Inconel 825 superalloy," International Journal of Data and Network Science, vol. 2, no. 3, pp. 79-88, 2018.

[13] H. Medellin, D. De Lange, J. Morales, and A. Flores, "Experimental study on electrodischarge machining in water of D2 tool steel using two different electrode materials," Proceedings of the Institution of Mechanical Engineers, Part B: Journal of Engineering Manufacture, vol. 223, no. 11, pp. 1423-1430, 2009.

[14] R. S. Bunker, "A review of shaped hole turbine film-cooling technology," J. Heat Transfer, vol. 127, no. 4, pp. 441-453, 2005.

[15] A. M. Titu and A. B. Pop, "Enhancing EDM Productivity for Plastic Injection Mold Manufacturing: An Experimental Optimization Study," Polymers, vol. 16, no. 21, p. 3019, 2024.

[16] G. Anbuchezhiyan, R. Saravanan, R. Pugazhenthi, K. Palani, and V. K. Mamidi, "Influence of coated electrode in nanopowder mixed EDM of Al–Zn–Mg–Si3N4 composite," Advances in Materials Science and Engineering, vol. 2022, no. 1, p. 9539790, 2022.

[17] L. Zhang, Y. Hu, S. Gong, and Z. Wang, "Experimental Study on the Comparison between Network Microstructure Titanium Matrix Composites and Ti6Al4V on EDM Milling," Materials, vol. 17, no. 10, p. 2282, 2024.

[18] I. Maher, L. H. Ling, A. A. Sarhan, and M. Hamdi, "Improve wire EDM performance at different machining parameters-ANFIS modeling," IFAC-PapersOnLine, vol. 48, no. 1, pp. 105-110, 2015.

[19] K. Ishfaq, M. Sana, M. Rehman, S. Anwar, A. Y. Alfaify, and A. W. Zia, "Role of biodegradable dielectrics toward tool wear and dimensional accuracy in Cu-mixed die sinking EDM of Inconel 600 for sustainable machining," Journal of the Brazilian Society of Mechanical Sciences and Engineering, vol. 45, no. 4, p. 235, 2023.

[20] M. Patel Gowdru Chandrashekarappa, S. Kumar, D. Y. Pimenov, and K. Giasin, "Experimental analysis and optimization of EDM parameters on HcHcr steel in context with different electrodes and dielectric fluids using hybrid taguchi-based PCA-utility and CRITIC-utility approaches," Metals, vol. 11, no. 3, p. 419, 2021.

[21] S. Shirguppikar, M. Patil, V. Ganachari, T. Kolekar, P. Jadhav, and A. Chougule, "Experimental investigation of CNT coated tools for EDM processes," Materials Today: Proceedings, vol. 5, no. 2, pp. 7131-7140, 2018.

[22] B. Fotovvati, N. Namdari, and A. Dehghanghadikolaei, "On coating techniques for surface protection: A review," Journal of Manufacturing and Materials processing, vol. 3, no. 1, p. 28, 2019.

[23] V. Sharun et al., "Study on developments in protection coating techniques for steel," Advances in Materials Science and Engineering, vol. 2022, 2022.

[24] R. Naveen Anthuvan and V. Krishnaraj, "Effect of coated and treated electrodes on Micro-EDM characteristics of Ti-6Al-4V," Journal of the Brazilian Society of Mechanical Sciences and Engineering, vol. 42, pp. 1-16, 2020.

[25] N. Ahmed, M. A. Hurairah, M. A. Ali, M. H. Raza, A. U. Rehman, and M. Rafaqat, "Impact analysis of electrode materials and EDM variables on the surface characteristics of SS316L for biomedical applications," journal of materials research and technology, vol. 27, pp. 3487-3505, 2023.

[26] Y. Q. Laibi and S. K. Shather, "Effect of SiC-Cu electrode on material removal rate, tool wear and surface roughness in EDM process," Engineering and Technology Journal, vol. 38, no. 9, pp. 1406-1413, 2020.

[27] A. S. Walia et al., "Surface roughness analysis of H13 steel during electrical discharge machining process using Cu–TiC sintered electrode," Materials, vol. 14, no. 20, p. 5943, 2021.

[28] D. Sharma and S. S. Hiremath, "Review on tools and tool wear in EDM," Machining Science and Technology, vol. 25, no. 5, pp. 802-873, 2021.

[29] T. R. Ablyaz, E. S. Shlykov, K. R. Muratov, and A. V. Zhurin, "Study of the EDM process of bimetallic materials using a composite electrode tool," Materials, vol. 15, no. 3, p. 750, 2022.

[30] C. Samantra, A. Barua, S. Pradhan, K. Kumari, and P. Pallavi, "Parametric Investigation of Die-Sinking EDM of Ti6Al4V Using the Hybrid Taguchi-RAMS-RATMI Method," Applied Sciences, vol. 14, no. 16, p. 7139, 2024.

[31] M. Bhaumik and K. Maity, "Effect of different tool materials during EDM performance of titanium grade 6 alloy," Engineering Science and Technology, an International Journal, vol. 21, no. 3, pp. 507-516, 2018.

[32] A.-H. Chiou, C.-C. Tsao, and C.-Y. Hsu, "A study of the machining characteristics of micro EDM milling and its improvement by electrode coating," The International Journal of Advanced Manufacturing Technology, vol. 78, pp. 1857-1864, 2015.

[33] K. E. Kitko and Q. Zhang, "Graphene-based nanomaterials: From production to integration with modern tools in neuroscience," Frontiers in systems neuroscience, vol. 13, p. 26, 2019.

[34] X. J. Lee et al., "Review on graphene and its derivatives: Synthesis methods and potential industrial implementation," Journal of the Taiwan Institute of Chemical Engineers, vol. 98, pp. 163-180, 2019.

[35] W. Meng and B. Gillispie, "Mechanical properties of Ti-containing and W-containing diamond-like carbon coatings," Journal of applied physics, vol. 84, no. 8, pp. 4314-4321, 1998.

[36] I. Taheridoustabad, M. Khosravi, and Y. Yaghoubinezhad, "Fabrication of GO/RGO/TiC/TiB2 nanocomposite coating on Ti–6Al–4V alloy using electrical discharge

coating and exploring its tribological properties," Tribology International, vol. 156, p. 106860, 2021.

[37] S. Peng, X. Fan, S. Li, and J. Zhang, "Green synthesis and characterization of graphite oxide by orthogonal experiment," Journal of the Chilean Chemical Society, vol. 58, no. 4, pp. 2213-2217, 2013.

[38] S. M. R. Sedehi, M. Khosravi, and Y. Yaghoubinezhad, "Mechanical properties and microstructures of reduced graphene oxide reinforced titanium matrix composites produced by spark plasma sintering and simple shear extrusion," Ceramics International, vol. 47, no. 23, pp. 33180-33190, 2021.

[39] H. Afshari, F. Taher, S. A. Alavi, M. Afshari, M. R. Samadi, and F. Allahyari, "Studying the effects of FDM process parameters on the mechanical properties of parts produced from PLA using response surface methodology," Colloid and Polymer Science, vol. 302, no. 6, pp. 955-970, 2024.

[40] M. Afshari, S. Bakhshi, M. R. Samadi, and H. Afshari, "Optimizing the mechanical properties of TiO2/PA12 nano-composites fabricated by SLS 3D printing," Polymer Engineering & Science, vol. 63, no. 1, pp. 267-280, 2023.

[41] R. R. Behera, S. Pal, and B. Nanda, "EDM machinability and surface characterisation of Al-SiC metal matrix composites: ANOVA based response surface study," Next Materials, vol. 11, p. 101715, 2026.

[42] K. Surani, M. Irfanul Haque Siddiqui, A. Kumar, and I. Ashraf, "The evaluation of machining performances and surface roughness of TZM-molybdenum superalloy processed by silicon carbide powder mixed EDM process using RSM and ANOVA," AIP Advances, vol. 14, no. 3, 2024.

[43] R. ÇAKIROĞLU, "Analysis of EDM machining parameters for keyway on Ti-6Al-4V alloy and modelling by artificial neural network and regression analysis methods," Sādhanā, vol. 47, no. 3, p. 150, 2022.

[44] D. C. Montgomery, Design and analysis of experiments. John wiley & sons, 2017.

[45] S. Bhowmick, R. Mondal, S. Sarkar, N. Biswas, J. De, and G. Majumdar, "Parametric optimization and prediction of MRR and surface roughness of titanium mixed EDM for Inconel 718 using RSM and fuzzy logic," CIRP Journal of Manufacturing Science and Technology, vol. 40, pp. 10-28, 2023.

[46] M. Dallakehnejad, H. Afshari, M. Lakhi, and M. R. Maraki, "Experimental Evaluation of EDM Parameters for MO40 Steel Using RSM and Thermal Heat-Flux Analysis," Science and Technology in Mechanical Engineering, pp. -, 2026.

[47] E. Selahshorrad et al., "Simultaneous optimization of the tensile strength, bending strength, hardness and wear resistance of WCu composite produced by sintering process," International Journal of Refractory Metals and Hard Materials, vol. 117, p. 106430, 2023.

Supplementary Files

This is a list of supplementary files associated with this preprint. Click to download.

- Tables.docx